

Chapter 2

Sublethal Environmental Stress

2.1 The Geological Record

The concept of sublethal environmental stress denotes specific conditions that are critical to the survival or normal development of living organisms. The most common cases of environmental perturbations include pollution or poisoning by chemicals such as toxic gases, nutriment shortage, large scale sea level falls, major climatic changes, hydric stress, acid rains, marine anoxies, etc. The origins of environmental stress can easily be identified and quite naturally the particular kind of stress can be hostile to some organisms and favourable to others.

The role of natural environmental stress on development and evolution is widely accepted (Badyaev 2005; Bijlsma and Loeschcke 2005; Nevo 2011; Kishony and Leibler 2003; Hoffman and Parsons 1991; Rutherford and Lindquist 1998; Hangartner et al. 2011; Cabej 2011; Jablonka and Raz 2009; Jablonka 2013; Schlichtling and Pigliucci 1998). The nature of sublethal environmental stress that occurred during major extinctions such as Permian-Triassic (PT), Triassic-Jurassic (TJ), Pliensbachian-Toarcian (PI-To) and Cretaceous-Tertiary (KT) is currently intensively investigated by means of geochemical and geochronological studies (see, for example, the data in Figs. 2.3 and 2.5.). However most problems related to these exceptional situations belong to the realm of palaeontology and most, if not all, of such palaeontological studies are dedicated to a census of the biodiversity variations (counting how many groups survive, how many disappear, etc.) rather than to the understanding of the basic phenotypic and epigenetic variations induced by major environmental perturbations. The modes of evolution during major extinction events, the characteristics of the organisms surviving major crises and what types of transformations have affected them have not been explored. The main goal of the present study is precisely to analyse in detail the transformations of some invertebrates during major extinction periods.

The geological record of environmental stress is naturally poor because local pollution, nutrient levels, paleotemperatures, etc. can hardly be deduced neither from sediments nor from fossils. The primary indication and proof of the sporadic sublethal environmental stress are the extinction periods themselves, which are easily recognized from the presence of major faunal turnovers reflecting the disappearance of entire phyla and their replacement by new ones (Sepkoski 1978; Benton 1995).

The classical explanations of the origins of extinctions include extraterrestrial impacts, marine regressions, climatic changes or anoxic events (Hallam and Wignall 1997; Hart 1996; Sepkoski 1978; Benton 1995; see also review by Courtillot and Gaudemer 1996). The theory of giant volcanism (Courtillot 1999) has the most general explanatory power, considering enormous potential consequences to the chemistry of seawater, global climate and temperatures. There is an almost perfect correlation between the major extinctions and periods of volcanism (Fig. 2.1, from Courtillot loc.cit.). Virtually all major extinctions are related to the major ecological instability generated by giant volcanism, i.e. climatic changes, atmospheric poisoning by sulfur gases, as well as by darkening generated by fine particles and aerosols inducing major coolings and fall in the sea level (Fig. 2.2). In extremes, for example, at the Permian-Triassic boundary, the only organisms found in crisis sediments are microbialites and fern or fungi spores. Often these sediments do not contain any fossils and hence are known as barren intervals. The after extinction recovery is generally characterized by the explosion of simple and primitive life forms, which can be divided into two major groups:

1. Persistent opportunistic simple forms such as bacteria, fungi, ferns and some simple forms or other microfossils.
2. Primitive-looking forms derived from their immediate ancestors by retrograde evolution (a phenomenon that has been described as proteromorphosis), often associated with a reduction in body size. These organisms are not Lazarus taxa because their absence in sediments older than the ones where they are found is fully reproducible worldwide and the duration of the intervals of time in which they are totally absent can last several millions or several tens of millions of years. In other words, a “Lazarus” explanation of such organisms cannot be reconciled with the geological record.

The present paper analyses how different groups (Foraminifera, Radiolaria, Ammonoids, Nautiloids, Corals, Conodonts and Silicoflagellids) of invertebrates (except conodonts) survive the sublethal biotic crises during extinction episodes and elaborates previously published works (Guex 1992, 1993, 2001; 2006). This study also aims at developing a model explaining the heterochronous repetition of similar evolutionary lineages without invoking repetitions of identical environmental conditions.

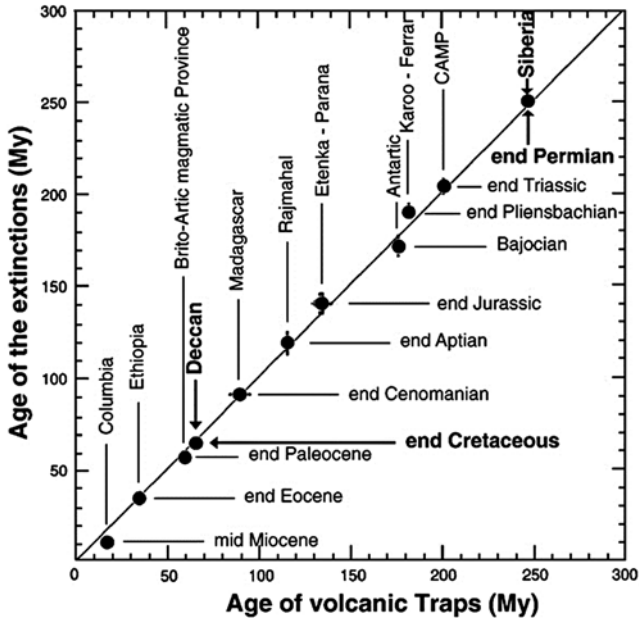


Fig. 2.1 Bivariate graph showing the correspondence between the principal mass extinctions and their geochronometrical age From Courtillot (1999), modified

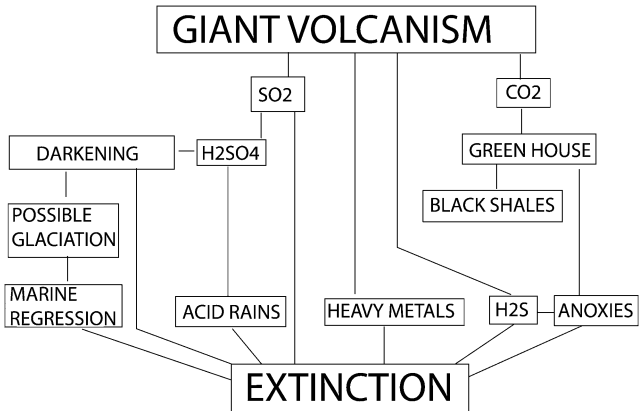


Fig. 2.2 Summary of the most obvious relationships between giant volcanism and major extinctions

2.2 Geochemistry, Geochronology and Volcanic Stress

2.2.1 Introduction

Two major extinctions generated by giant volcanism have been recently studied in detail by the author and his colleagues: the Triassic-Jurassic and the Pliensbachian-Toarcian boundaries. These two major geological events will be discussed in the following sections in light of recent geochemical and geochronological data and will illustrate the environmental framework of the retrograde evolutions observed during these events and discussed in Chaps. 4–6.

2.2.2 A Precise Timing of the End Triassic Extinction

The End Triassic Extinction has long been suspected to be related to the onset of the Central Atlantic Magmatic Province (CAMP) volcanism but it is only recently that U-Pb ages measured on zircons have allowed a precise correlation with the relative timescale based on the evolution of the ammonites. That correlation has been established based on very detailed stratigraphic research done in the American Cordilleras (Northern Peru and Nevada, USA) and on the discovery of ash beds deposited in the same levels as age diagnostic ammonites (Guex 1995; Schoene et al. 2010; Guex et al. 2012a). These discoveries allowed us to propose an original model explaining the precise timing of the End Triassic extinction (ETE) (Fig. 2.3).

One popular model to explain the ETE catastrophic event invokes super-greenhouse conditions due to extreme atmospheric CO₂ concentrations (McElwain et al. 1999; Schaller et al. 2011). This enrichment is often interpreted as degassing of magmatic CO₂ from huge volcanic basalt provinces (e.g. Sobolev et al. 2011 for the Permian-Triassic crisis) and/or from the degassing of carbonaceous or organic rich sediments (e.g. Svensen et al. 2009).

The second scenario invokes a short period of global icehouse conditions caused by degassing of huge volumes of volcanic SO₂, atmospheric poisoning, cooling and eustatic regression coeval with the main extinction (ETE) but probably older than the main basalt emissions. As mentioned above, this model uses the same arguments as those given in Sect. 2.2.3 for the Late Pliensbachian cooling event.

Although both hypotheses are compatible with massive volcanic degassing related to the emission of large volumes of flood basalts, they must also be able to explain the palaeontological record in complete stratigraphic sections that displays decoupling between the (marine) ammonoids vs. (terrestrial) plant extinctions (Guex et al. 2012a). Correlating the sedimentary and the fossil record with carbon and oxygen isotope variations and sea level changes from the T-J and PI-To boundaries indicates that both boundaries are related to a regressive event followed by major sea level rise (Guex et al. 2001, 2004, 2012a).

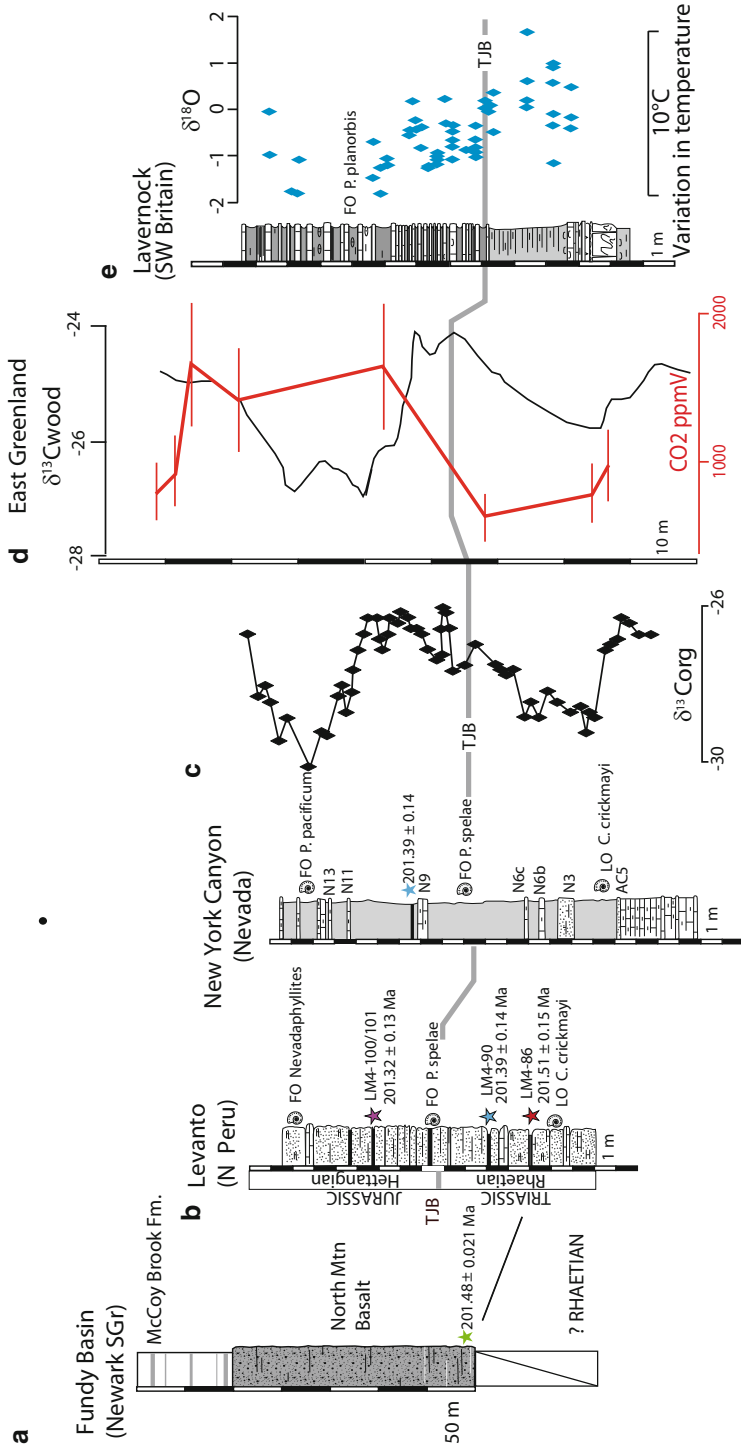


Fig. 2.3 (a–c) Numerical ages of the base of the North Mountain basalt and of the TJB in Peru and Nevada. δ¹³C curve at New York Canyon (Nevada). From Schoene et al. (2010), Guex et al. (2004) and Bartolini et al. (2012). (d) Variation of the CO₂ ppmV and δ¹³C in Greenland. Redrawn from McElwain et al. (2009). (e) Variation of the δ¹⁸O in SW Britain, numerical data by courtesy of Korte et al. (2009). Simplified from Guex et al. (2015)

The data allowing us to discuss the various hypotheses of recent extinction models and the timing concerning the End Triassic Extinction (ETE) and the T-J boundary is shown in Fig. 2.3 (for references see figure caption). This compilation synthesizes the timing of sea level changes, and $\delta^{13}\text{C}_{\text{org}}$, $\delta^{18}\text{O}$, and pCO_2 variations in relation with paleotemperatures, the age of the onset of the CAMP-related basaltic volcanism in the northeastern United States (Newark Supergroup) and Morocco (Argana Basin), and the ages of the two distinct End Triassic (ammonoids) and Earliest Jurassic (terrestrial plants) extinctions.

The chronology, established by ammonoids and U-Pb dating implies that the Newark supergroup basalts postdates the ETE and the disappearance of the latest Triassic ammonite *Choristoceras crickmayi* (Guex et al. 2004; Schoene et al. 2010). The delay between the recovery of the Jurassic ammonites and the extinction of the very last Triassic ammonoids lasted at least 200 kyr (probably more), based on sedimentary rates in Northern Peru and Nevada. The extinction of the last Triassic ammonoids in the uppermost Rhaetian is correlated with a strong negative excursion of $\delta^{13}\text{C}$ and a marine regression (Guex et al. 2004). The $\delta^{18}\text{O}$ record (Clemence et al. 2010; Korte et al. 2009) indicates a cooling episode, which could explain the regressive event recorded in the upper Rhaetian of Austria, England and Nevada. The initial regression is followed by a significant sea level rise potentially associated to large volcanic CO_2 emissions related to the CAMP basaltic volcanism (McElwain et al. 1999, 2009; Schaller et al. 2011; Bartolini et al. 2012). A major plant extinction is correlated with the greenhouse conditions that postdates the ETE by at least a few hundred thousand years. The plant extinction is recorded in Greenland (McElwain et al. 1999, 2009) and is associated with a second negative $\delta^{13}\text{C}$ recorded in the Hettangian *Psiloceras planorbis* beds (coeval with *P. pacificum*).

The recovery of the ammonites after the End Triassic extinction, calibrated with the geochronological data is illustrated in Fig. 2.4. This diagram shows a partial correlation between the $\delta^{13}\text{C}_{\text{org}}$ curve and the diversity fluctuations. This figure shows that the well-known first negative excursion of the organic carbon is correlated with the peak of the Rhaetian extinction.

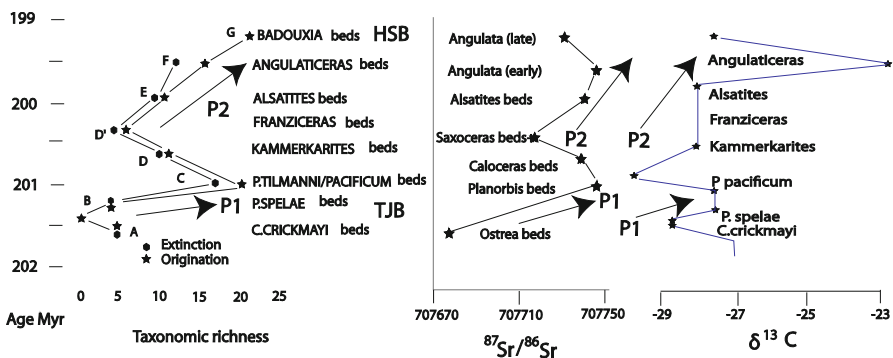


Fig. 2.4 Variations of the taxonomic richness of the ammonites and variations of $\delta^{13}\text{C}_{\text{org}}$ and $\text{Sr}^{87/86}$, from Guex et al. (2012a). P1 and P2: positive pulses of the carbon isotopes. TJB and HSB: Triassic Jurassic Boundary and Hettangian Sinemurian Boundary

The second negative excursion is restricted to the Psiloceras zone. The mid-Hettangian slow-down of the diversification is followed by an explosion of the diversity in the Upper Hettangian and by a new positive excursion of the organic carbon. However we note that the minimum of the ammonite diversity (D') occurs later than the minimum of the $\delta^{13}\text{C}_{\text{org}}$ curve which is located between the *P. pacificum* and *Kammerkarites* beds. The strontium data, based on Jones et al. (1994) measurements in Great Britain (see also Cohen and Coe 2007) are plotted as the mean-values of the original measurements per subzone. There is an apparent correlation between the taxonomic richness and the variation of the $^{87}\text{Sr}/^{86}\text{Sr}$ ratio. Such a correlation was already observed and discussed by Cardenas and Harries (2010) at a very large scale in the marine Phanerozoic genera. According to these authors, this correlation is basically controlled by the availability of marine nutrients.

2.2.3 *The Pliensbachian -Toarcian Extinctions*

A model similar to the one presented above (Fig. 2.3) can be proposed for the Pliensbachian Toarcian crisis which is known to be correlated with the onset of the Karoo-Ferrar large igneous province (Palfy and Smith 2000).

Recent high precision U-Pb dating on zircons of major sill intrusions in the Karoo basin can be directly correlated with the well-known Toarcian Oceanic Anoxic Event (OAE) and is concomitant with these sill intrusions into organic rich sediments of that basin (Guex et al. 2012b; Sell et al. 2014). In Fig. 2.5, we present a synthesis of major isotopic variations, the available geochronological data and major sea level variations. These data allow us to investigate whether and how the geochemical and biochronological data can be correlated with the magmatic activity of the Karoo-Ferrar LIP.

The end-Pliensbachian extinction, preceding the Toarcian AOE by a few hundred kyr (Dera et al. 2010), is marked by an important diversity drop (disappearance of 90 % of the ammonite taxa) associated with a generalized sedimentary gap linked to a marked regression event in NW-Europe and the Pacific area.

This regression was interpreted as being due to a major short lived glaciation (Guex et al. 2001, 2012b) coeval with the main extinction and preceding the main basalt eruptions. Our major arguments refer to an important emersion topography observed on seismic images of the North Sea (Marjanac and Steel 1997), to the evidence of polar ice storage (Price 1999) and to the deposition of thick conglomerates (Dunlap Formation in Nevada (USA) (Muller and Ferguson 1939) and Ururoa-Kawhia area, New Zealand (Hudson 2003)). The cooling model is supported by recent $\delta^{18}\text{O}$ data on belemnites (Gómez et al. 2008; Harazim et al. 2012) and by the discovery of glendonites in the upper part of the Pliensbachian (Suan et al. 2011). The origin of the major cooling is probably related to huge volcanogenic SO_2 degassing during the Late Pliensbachian preceding the major CO_2 emissions of the Early Toarcian (Guex et al. 2001).

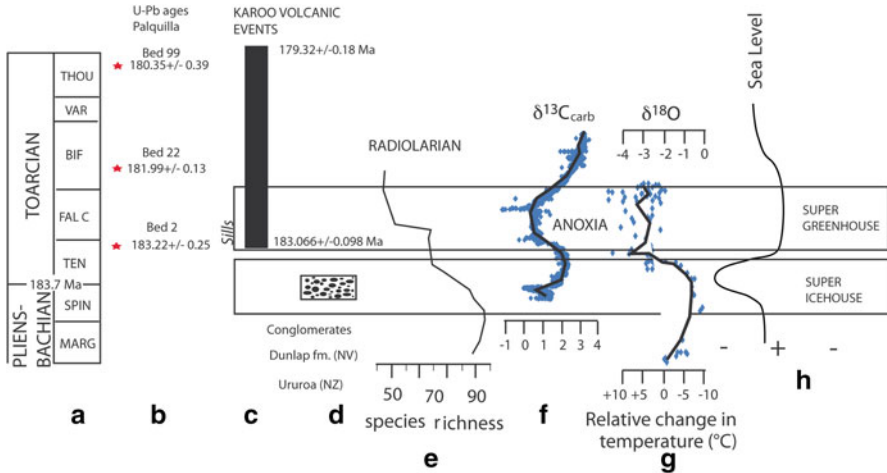


Fig. 2.5 A model for the Pliensbachian-Toarcian crisis. (a) Standard ammonite zonation of the Upper Lias. (b, c) Numerical ages of beds 2, 22 and 99 at Palquilla (Peru) and of the Karoo basalts. Redrawn from Guex et al. (2012b), Sell et al. (2014). (d) Conglomerates present at the Pliensbachian—Toarcian boundary in New Zealand and Nevada. From Guex et al. (2012b). (e) Species richness of Radiolarians in the Upper Pliensbachian and Early Toarcian. From Gorican et al. (2013). (f) Variation of the $\delta^{13}\text{C}$ around the Pliensbachian—Toarcian boundary. Redrawn from Hesselbo et al. (2007). (g) Variation of the $\delta^{18}\text{O}$ and paleotemperatures around the Pliensbachian—Toarcian boundary. Redrawn from Dera et al. (2010). (h) Variations of sea level around the Pliensbachian—Toarcian boundary. From Guex et al. (2001) and simplified from Guex et al. (2015)

The regressive phase is followed, after a few hundred thousand years, by a world-wide transgression during the Early Toarcian, with the deposition of black shales associated with the Toarcian OAE (Jenkyns 1988). The Toarcian OAE itself is responsible for a second extinction affecting mainly benthic foraminifera populations (Bartolini et al. 1990) and brachiopods (García-Joral et al. 2011). Radiolarians were also affected (Fig. 4.5) but their extinction was apparently slightly delayed in comparison with benthos and probably coincided with a drastic fertility drop just after the OAE.

The succession of ice house conditions immediately followed by super greenhouse conditions can be explained thanks to a petrological model elaborated by our colleagues Sebastien Pilet and Othmar Muntener to explain the SO_2 dominated vs. CO_2 dominated degassing couplet generating the successive cold and hot conditions. The model invokes a thermal erosion of the cratonic lithosphere inducing giant $\text{H}_2\text{S}/\text{SO}_2$ release from sulfur bearing basal continental crust before CO_2 becomes the dominant gas associated to the giant basalt emission (Guex et al. 2015b).

2.3 Graphic Representation of the Relationships Between Stress, Time and Evolutionary State

The catastrophe theory is a domain of the differential topology which was invented by René Thom (1972). It aims at building the simplest continuous dynamic model which can generate a morphology, given empirically, or a set of discontinuous phenomena.

Thom's theory concerns the phenomena where a gradual and relatively slow change produces a sudden jump of the state of the system. Such phenomena are called catastrophes. The graphical representation known under the name of "cusp catastrophe" is ideal to describe empirically the cases of the evolutionary jumps which arise during gradual changes in the environmental stress (Fig. 2.6). The surface illustrated in Fig. 2.3 represents the variable which characterizes the more or less advanced state of a taxonomic group which varies during the evolutionary time. This state is controlled by two parameters which, in our case, are the environmental stress and the time factor.

When these parameters vary, the curve of the state of the taxonomic group under study follows a trajectory which depends on time and on the intensity of the environmental stress. When the stress gradually reaches a certain threshold, the evolutionary state of the evolving system arrives at the border of the cusp and a jump occurs towards a previous state of more primitive aspect. In this book we will use such simple diagrams to describe the phenomena of retrograde evolution.

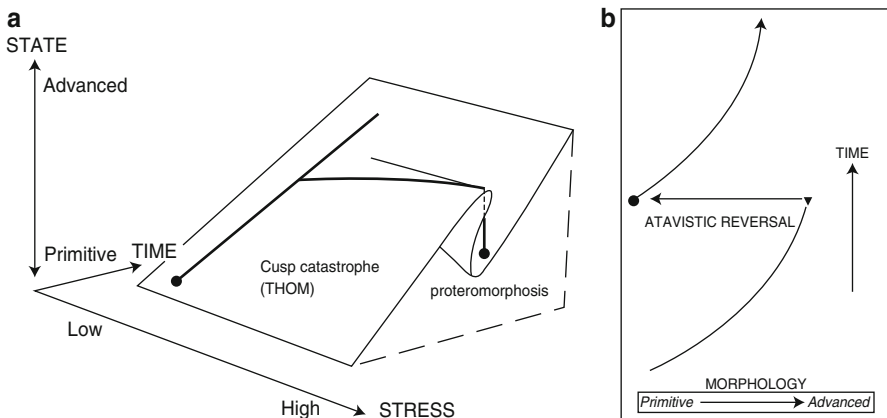


Fig. 2.6 The cusp catastrophe of Thom. (a) Stress and time are the parameters controlling the state of the evolving system (primitive–advanced). (b) Simplified graphic representation of (a)